AD-A041 509 YESHIVA UNIV NEW YORK F/G 20/12
STUDY OF THE PHASE TRANSITION IN NIOBIUM DIOXIDE.(U)
1977 P M RACCAH DAA629-76-G-0168
UNCLASSIFIED ARO-13663.1-PX NL

| OF |
AD
A041509

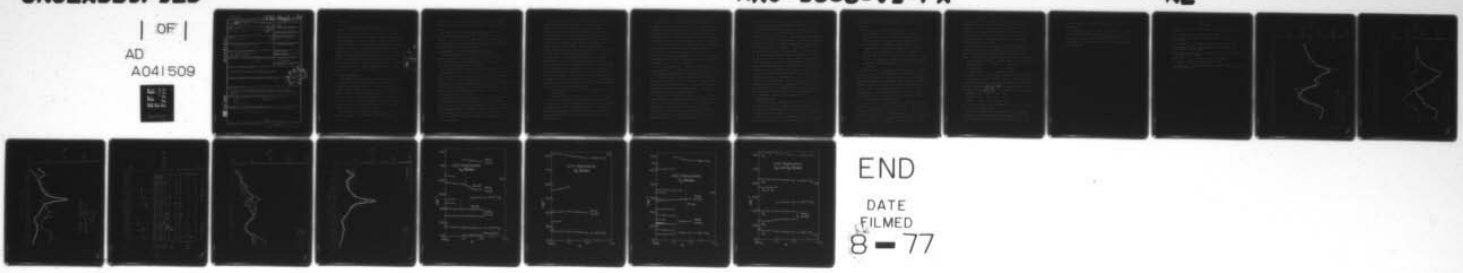

END
DATE
FILMED
8-77

Unclassified

SECURITY CLASSIFICATION OF THIS PAGE (When Data Entered)

ARO-13663.1-PX

REPORT DOCUMENTATION PAGE

READ INSTRUCTIONS BEFORE COMPLETING FORM

1. REPORT NUMBER: ARO-13663.1-PX	2. GOVT ACCESSION NO.
3. RECIPIENT'S CATALOG NUMBER	
4. TITLE (and Subtitle): STUDY OF THE PHASE TRANSITION IN NIOBIUM DIOXIDE,	5. TYPE OF REPORT & PERIOD COVERED: Final Report: 1 Apr 76 - 31 Mar 77
	6. PERFORMING ORG. REPORT NUMBER
7. AUTHOR(s): Paul M. Raccah	8. CONTRACT OR GRANT NUMBER(s): DAAG29-76-G-0168
9. PERFORMING ORGANIZATION NAME AND ADDRESS: Yeshiva University, New York, New York 10033	10. PROGRAM ELEMENT, PROJECT, TASK AREA & WORK UNIT NUMBERS
11. CONTROLLING OFFICE NAME AND ADDRESS: U. S. Army Research Office, Post Office Box 12211, Research Triangle Park, NC 27709	12. REPORT DATE: 1977
	13. NUMBER OF PAGES: 20
14. MONITORING AGENCY NAME & ADDRESS (if different from Controlling Office)	15. SECURITY CLASS. (of this report): Unclassified
	15a. DECLASSIFICATION/DOWNGRADING SCHEDULE

16. DISTRIBUTION STATEMENT (of this Report)

Approved for public release; distribution unlimited.

17. DISTRIBUTION STATEMENT (of the abstract entered in Block 20, if different from Report)

18. SUPPLEMENTARY NOTES

The findings in this report are not to be construed as an official Department of the Army position, unless so designated by other authorized documents.

19. KEY WORDS (Continue on reverse side if necessary and identify by block number)

Niobium compounds
Oxides
Phonons
Titanium oxides
Phase transformations
Energy bands

20. ABSTRACT (Continue on reverse side if necessary and identify by block number)

Results are presented on the electronic bands of NbO_2^T and $Nb_{(1-x)}^{T}{}_{y}O_2^{T}$ and on the phonon structure at K=0.

383 050

DD FORM 1 JAN 73 1473 EDITION OF 1 NOV 55 IS OBSOLETE

Unclassified

SECURITY CLASSIFICATION OF THIS PAGE (When Data Entered)

A. Introduction

It has long been recognized that the coupling of the cations, via homopolar bonding of the d-electrons, along the preferred c-axis direction plays a crucial role in the SCM transition mechanism.[1] We have tried to identify the p-d and d-d interband transitions in NbO_2 by comparing its normal incidence reflectivity spectra to that of TiO_2. As was shown earlier,[2] the structure of NbO_2 in the semiconducting phase, albeit slightly distorted, is tetragonal as is that of TiO_2 and in first approximation, one would expect that the spectra would look similar except for the d-band's contributions. Such a simple-minded assumption would also lead one to expect the main differences to show in the spectra where the light polarization is parallel to the c-axis.

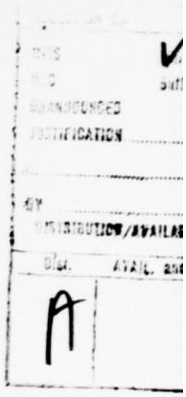

B. Optical Spectroscopy

The possibility of doping high quality NbO_2 single crystals with TiO_2[3] suggested another approach. Since Ti^{4+} has no d-electrons, each substitution of a Ti^{4+} for an Nb^{4+} would actually break a Nb-Nb pair and leave the lone Nb^{4+} ion with a dangling d-bond. Two consequences would follow. The first is that the conductivity and the magnetic moment at a fixed temperature would increase with the Ti^{4+} concentration and the second is that the optical spectra would be affected mostly where the d-band's contributions dominate.

We have fully carried out these experiments and the results have been accepted for presentation at the International

Semiconductor Conference (Rome, 1976), they will appear shortly in the proceedings. Only the salient features will be discussed below.

The large single crystals of NbO_2 and $Nb_{1-x}Ti_xO_2$ used in our measurements were grown[3] by the Czochralski-Kyropoulos technique in a tri-arc furnace built after the original design of Dr. Thomas B. Reed (M.I.T., Lincoln Laboratory); the procedure followed was outlined earlier (see Ref. 5).

B-1. Comparison of the NbO_2 and TiO_2 Optical Spectra

The normal incidence reflectivity of NbO_2 and TiO_2 was measured on oriented single crystals using polarized light. The instrument was a rotating light pipe reflectometer of the type originally designed by Dr. G. Rubloff.[4]

Let us consider first the spectra obtained with light polarization E parallel to the a-axis (Fig. 1). For the sake of convenience, we have shifted the entire NbO_2 spectrum to the left by approximately 0.7 eV. If one excepts the low energy maximum in the NbO_2 trace, the similarity between the spectra is quite conspciuous. This result is consistent with the assumption made earlier and identifies the first extremum in the NbO_2 (E || a-axis) spectrum as resulting from a d-d transition.

Let us now turn our attention to the E || c-axis spectra. Since the d-orbitals are along the c-axis, this is where we would expect to see strong differences between NbO_2 and TiO_2 according to the hypothesis mentioned earlier. The results shown in Fig. 2 are self-explanatory. No amount of shifting of either curve is going to bring about the kind of coincidence exhibited in the E || a-axis case.

In order to pursue further our discussion, we now need to perform a Kramers-Kronig analysis of our measurements and obtain the ε_2 (imaginary part of the frequency dependent dielectric constant) spectrum which usually exhibits maxima in reasonable agreement with the extrema in the joint density of states spectrum. However, such an analysis often suffers from a lack of information about strong oscillators lying outside the experimental range. We have palliated this difficulty by measuring the angular dependence of the reflectivity at a few selected wavelengths corresponding to our Ar^+ and Kr^+ ion laser lines. These measurements allowed us to compute independently ε_1 and ε_2 at a few predetermined frequencies. By forcing the result of the Kramers-Kronig analysis to pass through these independently obtained values of ε_1 and ε_2 one confers a degree of uniqueness and dependability to the transformation. The results are shown in Fig. 3 for pure NbO_2 and the location of interband transitions are indicated by arrows. The considerations presented earlier lead to a tentative set of assignments shown in Fig. 4 and to the following possibilities:

- The direct band gap of 0.8 eV is a_{1g} bonding to a^*_{1g} antibonding
- The transitions at 0.8, 1.5, 2.5 and 3.8 eV are d to d.

The first observation is actually quite interesting because it explains the significant anisotropy observed in the conductivity of single crystal NbO_2.[5] The second observation informs us as to the actual hierarchy of d-orbitals sublevels. This information is essential to the derivation of a reliable model for the SCM transition.

Fig. 8

B-2. Dependence of the NbO_2 Optical Spectrum on Ti Doping

We have measured the normal incidence reflectivity spectra of $Nb_{1-x}Ti_xO_2$ with x = 0.0, 0.05 and 0.20. X-ray and Raman measurements[7] have shown that for $x > 0.17$, the SCM transition is eliminated and the material has the undistorted rutile structure. Our reflectivity measurements therefore, straddle the SCM transition using Titanium doping instead of temperature. In Fig. 5, we show ε_2 (E || to c-axis) for all three compositions. It is quite clear that at least two interband transitions indicated by the arrows and located at 2.5 and 3.8 eV are affected by titanium doping and the effect is a steady displacement toward higher energies; implying, that titanium doping increases the a_{1g} - ($e_g\pi$,$e_g\sigma$) splitting.

In Fig. 6, we present the ε_2 dependence on Ti doping with light polarization E || a-axis. By and large, the only effect is the expected broadening due to disorder, except for the peak at 1.5 eV which increases with Ti concentration. This is not surprising as the peak at 1.5 eV is the only d-d transition observed with light polarization E ||to a-axis. Of course, these assignments are only a guess but they are internally consistent and therefore quite plausible.

The result of this analysis is simple. At this point, we already know that the SCM transition in NbO_2 results from a type of configurational instability. This is shown not only by the neutron diffraction work, but also by the optical spectroscopy results. They seem to indicate that the direct gap is bonding a_{1g} to antibonding a^*_{1g}. This type of gap is usually of the order of 3 eV as for instance in Ti_2O_3;[6] here

we have measured it to be 0.8 eV. This unusual result suggests a very simple explanation for the SCM transition. It results from the fact that, similar to Ti_2O_3, cation-cation pairs are formed via homopolar hybridization of d-orbitals preferentially along the c-axis. This, in turn, requires a slight displacement of the O^{--} providing a proper Coulombic potential and locking-in a stable configuration. However, contrary to Ti_2O_3, pairs here are contiguous and not separated by a vacancy and it is easy to see that two contiguous Nb ions bound to two other Nb ions in two different pairs could choose to break away from their partners and form a new pair. The only obstacle would be the oxygen rearrangement necessary to accomodate the new situation. The optical results suggest, as one possibility, that the energy needed for such a rearrangement is of the order of 0.8 eV. Now a look at the actual value of oxygen distortions will be most convincing as they are extremely small, in fact, at the limit of accuracy of X-ray techniques. Clearly, there will be a finite temperature at which the mean square amplitude of vibration of the oxygen ions will be comparable to the distortion itself at which point the difference between the two configurations will vanish provoking a collapse of the direct band gap.

C. Raman Spectroscopy

Our previous work, consistently with the results of Tanaka,[8] had shown that Ti doping lowered the transition temperature Tc and that by 17 atomic percent of Ti the material has a metallic conductivity at room temperature. This opened up the possibility of inducing the phase change at ambient by varying x in $Nb_{1-x}Ti_xO_2$ and following the process by Raman scattering. In performing

this experiment, which has been reported at the annual solid state meeting of the APS in March 1977, we fully realize its limitation.

a. Ti substitution would simulate temperature only if the determinant factor in the semiconductor to metallic transition mechanism is a pair breaking process instead of a tunneling excitation or a charge density wave.

b. At room temperature, NbO_2 has the C_{4h} symmetry and 32 molecules per unit cell while above Tc it has the D_{4h} symmetry and 2 molecules per unit cell; from which it follows that the $\underline{k}$ of the transformation is different from zero and we should not expect to see a Raman mode soften as we go from the distorted C_{4h} phase to the undistorted D_{4h} phase.

On the other hand, it was established earlier that the transition is of the second kind[9] and passing from one phase to the other does not generate an entirely new set of phonon branches. Simply the distorted phase exhibits a large number of phonons (actually symmetry indicates that we should expect 54 phonons, 18 Ag + 18 Bg + 18 Eg) because of a multiple folding of the Brillouin zone. As the material undergoes the phase transition, the Brillouin zone unfolds and all but four phonon branches (A_1g, B_1g, B_2g and Eg) should disappear.

In Figs. 7,8,9 and 10, we present the evolution of the Raman spectra in $Nb_{1-x}Ti_xO_2$ system as a function of x. The polarization selection rules are fairly well obeyed and Fig. 7 shows the Ag modes (ZZ polarization), Fig. 8 shows the Eg modes (XZ polarization), Fig. 9 shows the Bg modes (XY polarization), finally Fig. 10 (XX polarization) shows simultaneously Ag and Bg modes. Obviously

we are not seeing all the Raman active mode, in fact, we are barely able to detect half of them, but the information seems sufficient. In order to interpret the data, one should keep in mind that we are dealing here with an alloy and that we should expect to observe, in the undistorted rutile phase, all the TiO_2 modes in addition to the modes corresponding to the high symmetry rutile NbO_2.

As can be seen, the multiplicity of modes, present in the distorted pure NbO_2 phase, is reduced very fast and by x=0.1 already the spectra is dominated by the TiO_2 and NbO_2 (rutile) lines. If one excludes the TiO_2 rutile lines, one is left with -

ZZ polarization 125 cm^{-1}, 350 cm^{-1}, 390 cm^{-1}, 540 cm^{-1} and 730 cm^{-1}

XZ polarization 240 cm^{-1}, 390 cm^{-1}

XY polarization , 390 cm^{-1}

XX polarization 350 cm^{-1}, 390 cm^{-1}

Out of these four (125 cm^{-1}, 390 cm^{-1}, 540 cm^{-1}, and 730 cm^{-1}) are in a constant ratio to the four TiO_2 phonons. Since the phonons in the rutile structure are due to oxygen motions only, one does not expect scaling by $\left(\frac{\text{mass of Nb}}{\text{mass of Ti}}\right)^{\frac{1}{2}}$ but rather by a ratio of the spring constants $\left[\frac{K(Nb\text{-}O)}{K(Ti\text{-}O)}\right]^{\frac{1}{2}}$. The comparison is shown below

$NbO_2(cm^{-1})$	125	390	537	826
$TiO_2(cm^{-1})$	143	447	612	726
Ratio	1.144	1.146	1.140	1.138

and the results point out that Nb-O has a weaker spring constant than Ti-O as one would expect.

The two other modes at 240 and 350 cm^{-1} are particularly interesting as they belong neither to NbO_2 rutile nor to TiO_2 rutile. Since these modes are already dominant by x=0.12, we

intend to investigate them more closely as a function of temperature.

In conclusion, the work to date has informed us extensively on the electronic bands of NbO_2 and $Nb_{1-x}Ti_xO_2$ as well as on the phonon structure at K=0. These results will be used as a stepping stone to analyze the neutrons and magnetic results now in progress.

References

1. J. B. Goodenough,"Magnetism and the Chemical Bond", Wiley ed. (1956)

2. B. O. Marinder, Arkiv Kemi, 19, 435 (1963)

3. S. H. Shin, T. H. Halpern, and P. M. Raccah, Mat. Res. Bull. 10, 1061 (1975)

4. V. Gerhardt and G. W. Rubloff, Appl. Optics, 8, 305 (1969)

5. G. Belanger, J. Destry, G. Perluzzo, and P. M. Raccah, Can. Jour. Phys. 52, 2272 (1974)

6. S .H. Shin, F. H. Pollak, T.H. Halpern, and P. M. Raccah, Solid State Com. 16, 687 (1975)

7. S. H. Shin, F. H. Pollak, P. M. Raccah, unpublished

8. K. Sakata, J. Phys. Soc. Jap., 26, 582 (1969)

9. S. M. Shapiro, J. D. Axe, G. Shirane and P.M. Raccah, Solid State Comm. 15, 377 (1974)

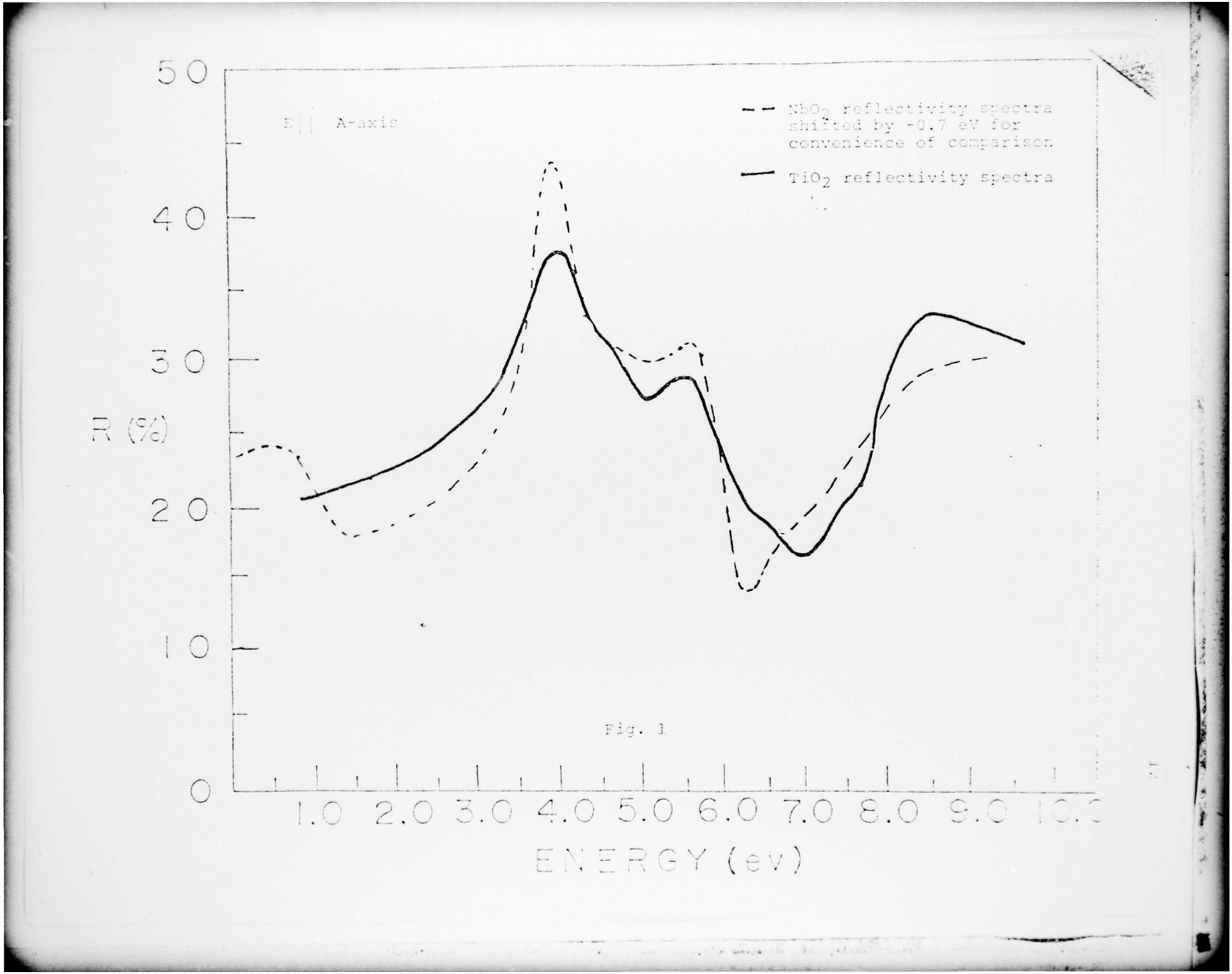
E|| A-axis
NbO_2 reflectivity spectra shifted by -0.7 eV for convenience of comparison
TiO_2 reflectivity spectra
R (%)
50
40
30
20
10
0
1.0 2.0 3.0 4.0 5.0 6.0 7.0 8.0 9.0
ENERGY (ev)

Fig. 1

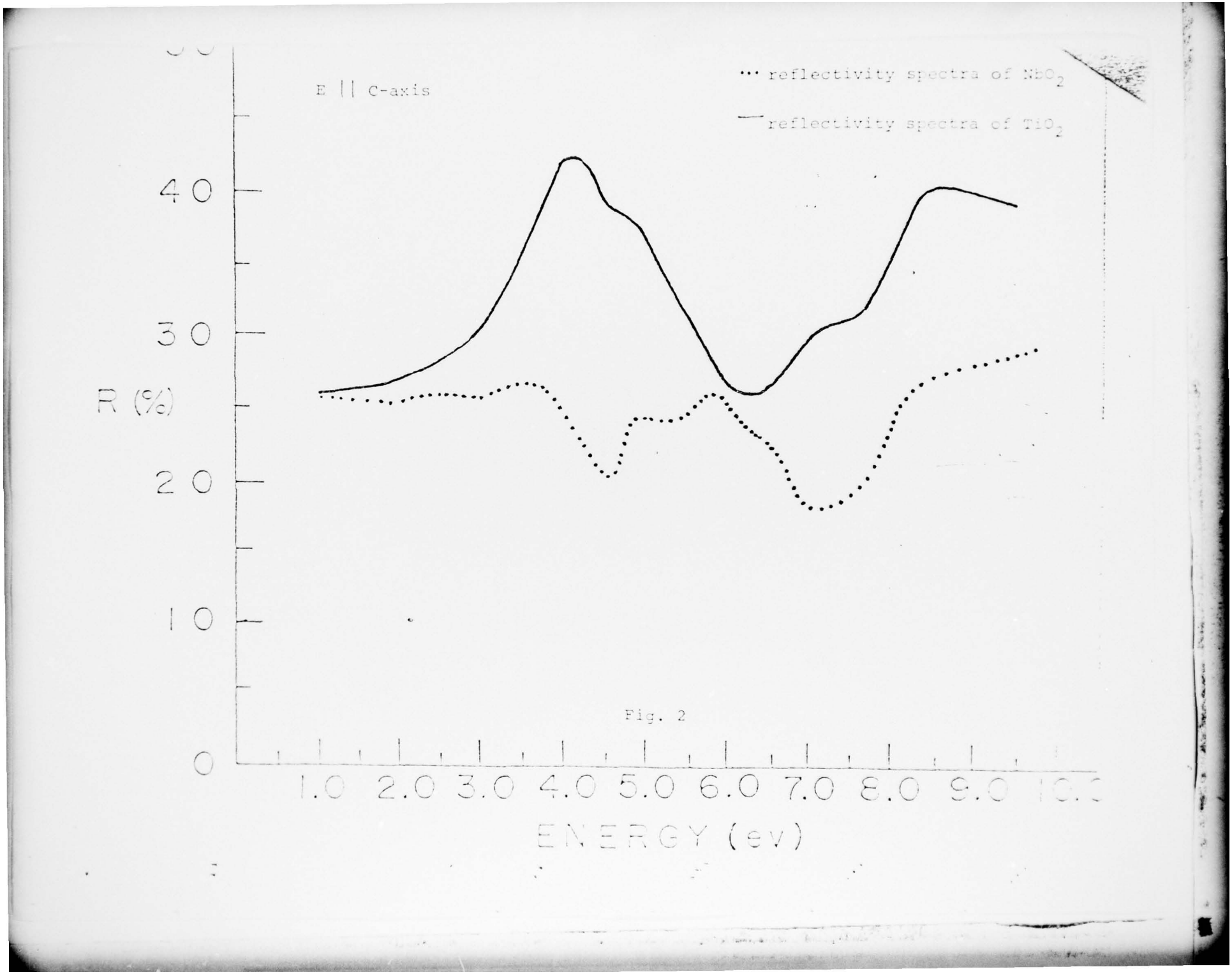
E || C-axis
··· reflectivity spectra of NbO_2
— reflectivity spectra of TiO_2
40
30
R (%)
20
10
0
1.0 2.0 3.0 4.0 5.0 6.0 7.0 8.0 9.0
ENERGY (ev)

Fig. 2

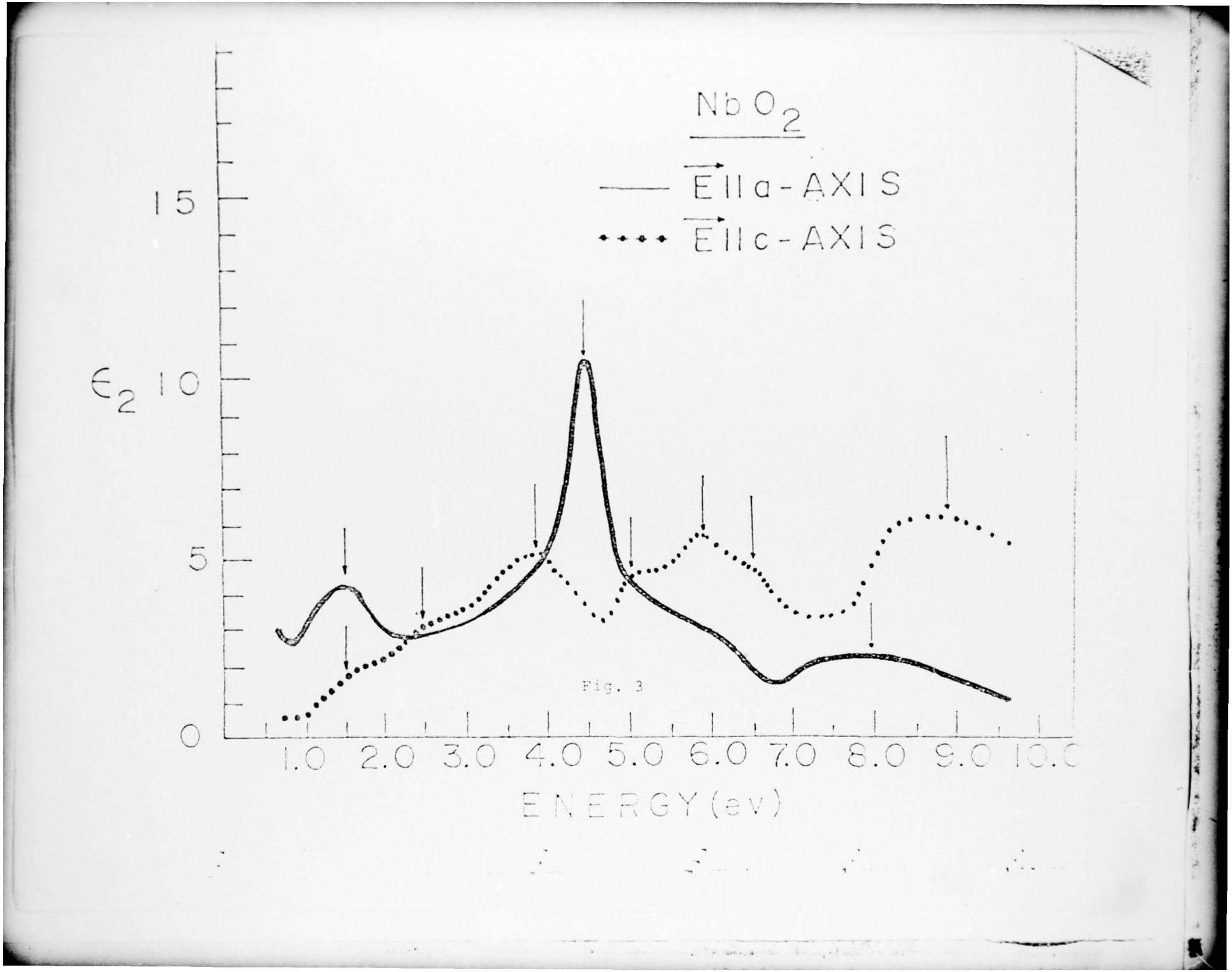
NbO2
Ella-AXIS
Ellc-AXIS
15
10
5
0
ε2
1.0
2.0
3.0
4.0
5.0
6.0
7.0
8.0
9.0
10.0
ENERGY(ev)

Fig. 3

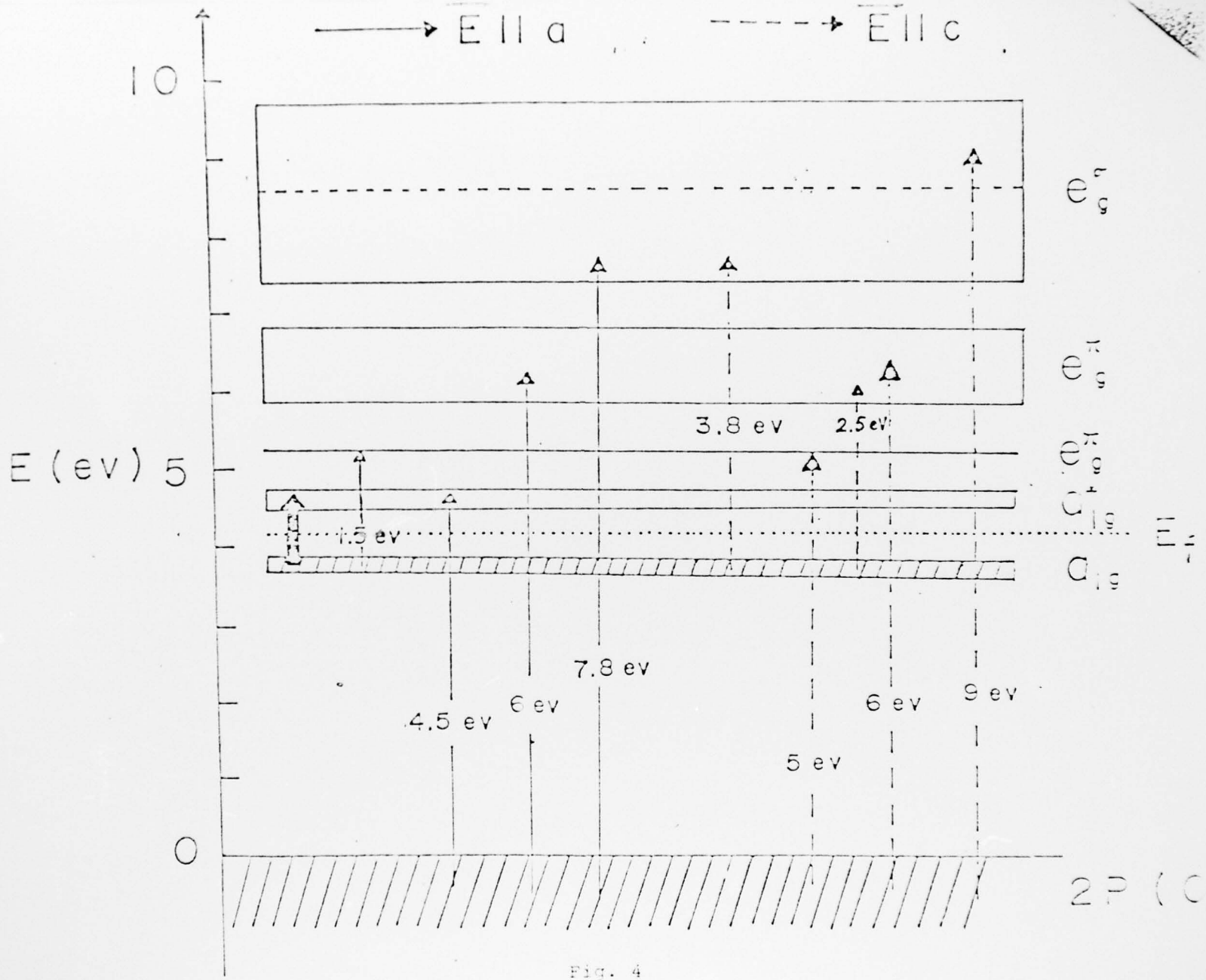

Fig. 4

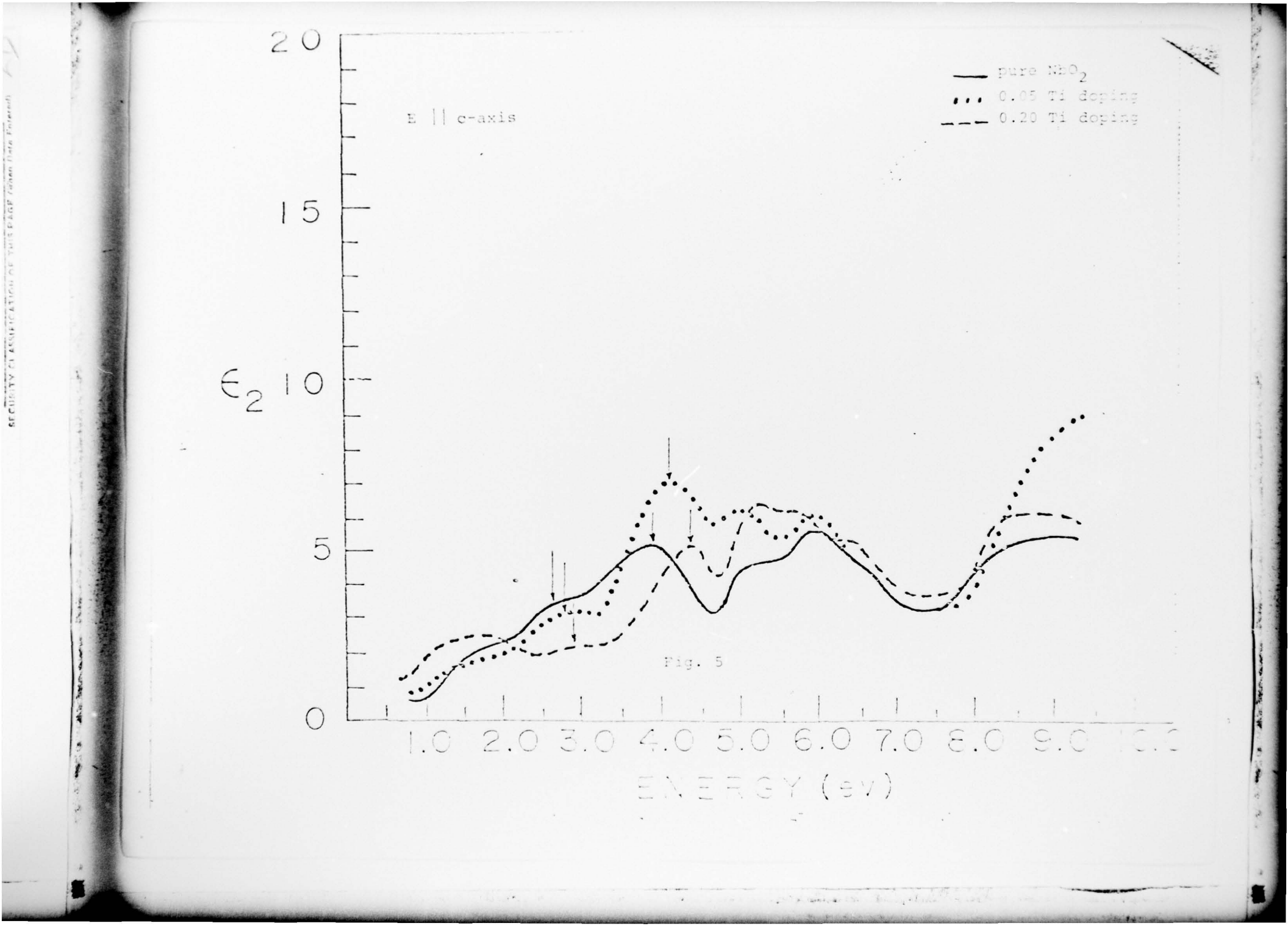
20
15
10
5
0
ϵ_2
E || c-axis
pure NbO_2
0.05 Ti doping
0.20 Ti doping
1.0
2.0
3.0
4.0
5.0
6.0
7.0
8.0
9.0
ENERGY (eV)

Fig. 5

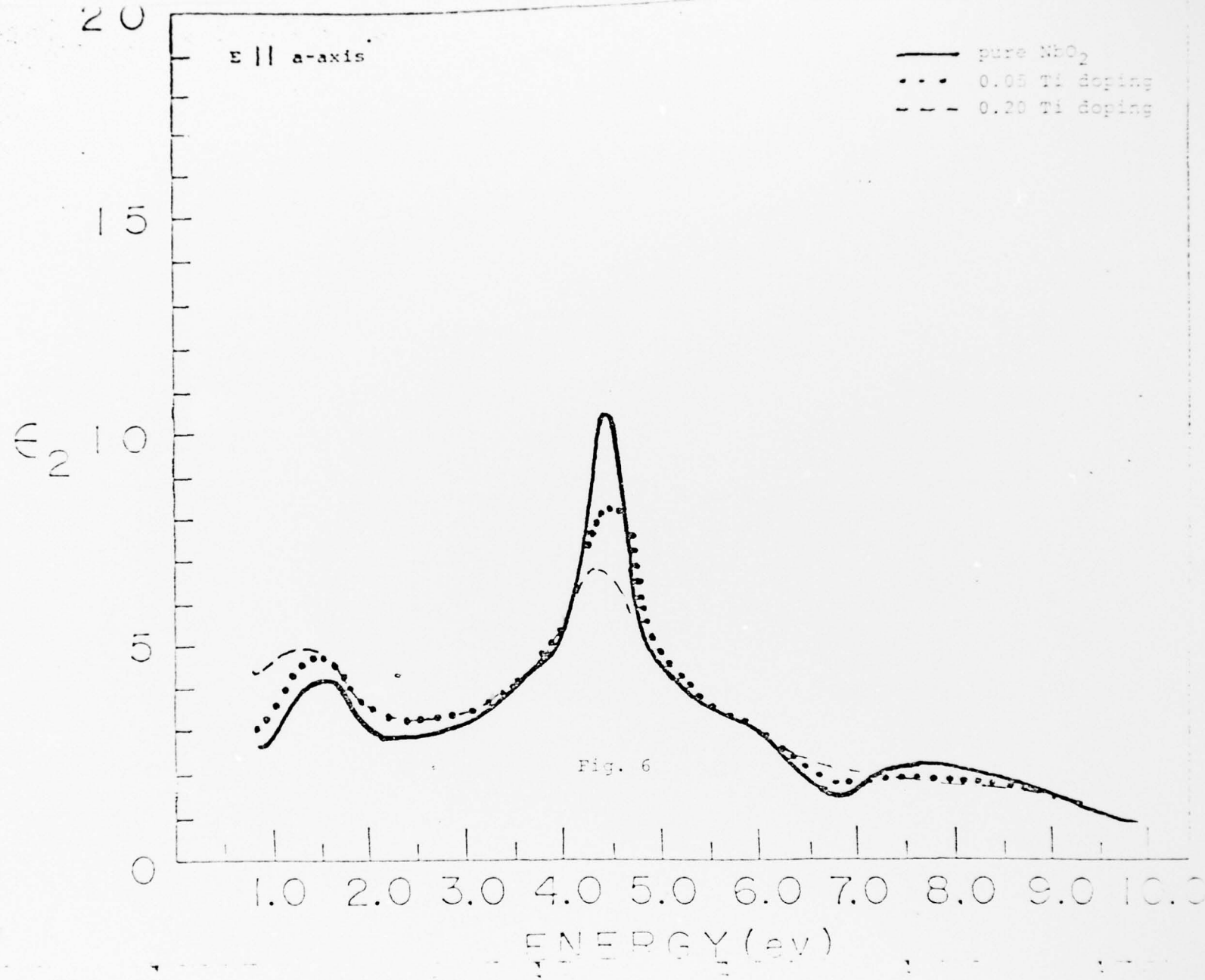
ε || a-axis
pure NbO_2
0.05 Ti doping
0.20 Ti doping
ϵ_2
20
15
10
5
0
1.0 2.0 3.0 4.0 5.0 6.0 7.0 8.0 9.0 10.0
ENERGY(ev)

Fig. 6

Fig. 7

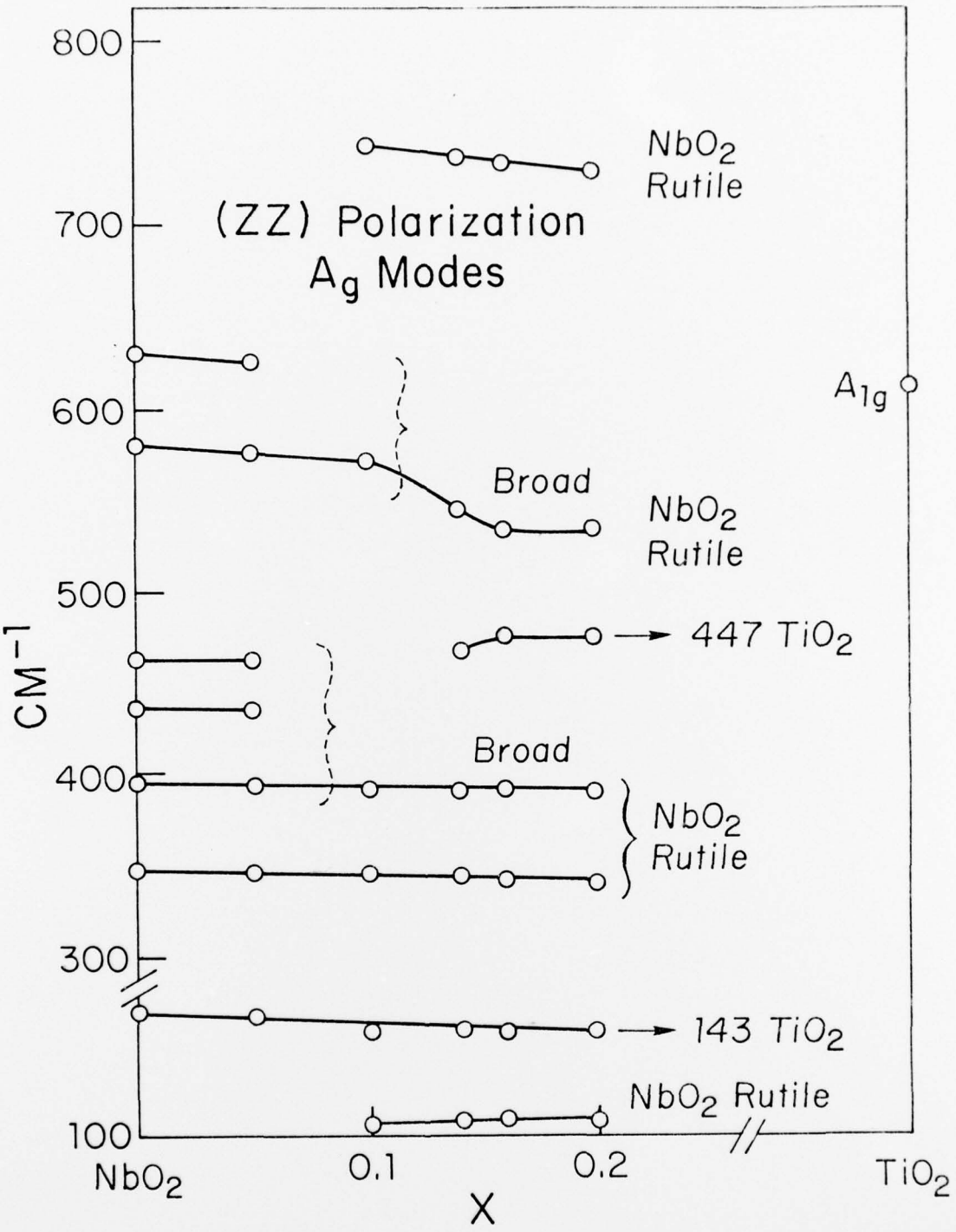
800
700
600
500
400
300
100
CM⁻¹
(ZZ) Polarization
Ag Modes
NbO2
Rutile
A1g
Broad
NbO2
Rutile
447 TiO2
Broad
NbO2
Rutile
143 TiO2
NbO2 Rutile
NbO2
0.1
0.2
TiO2
X

Fig. 8

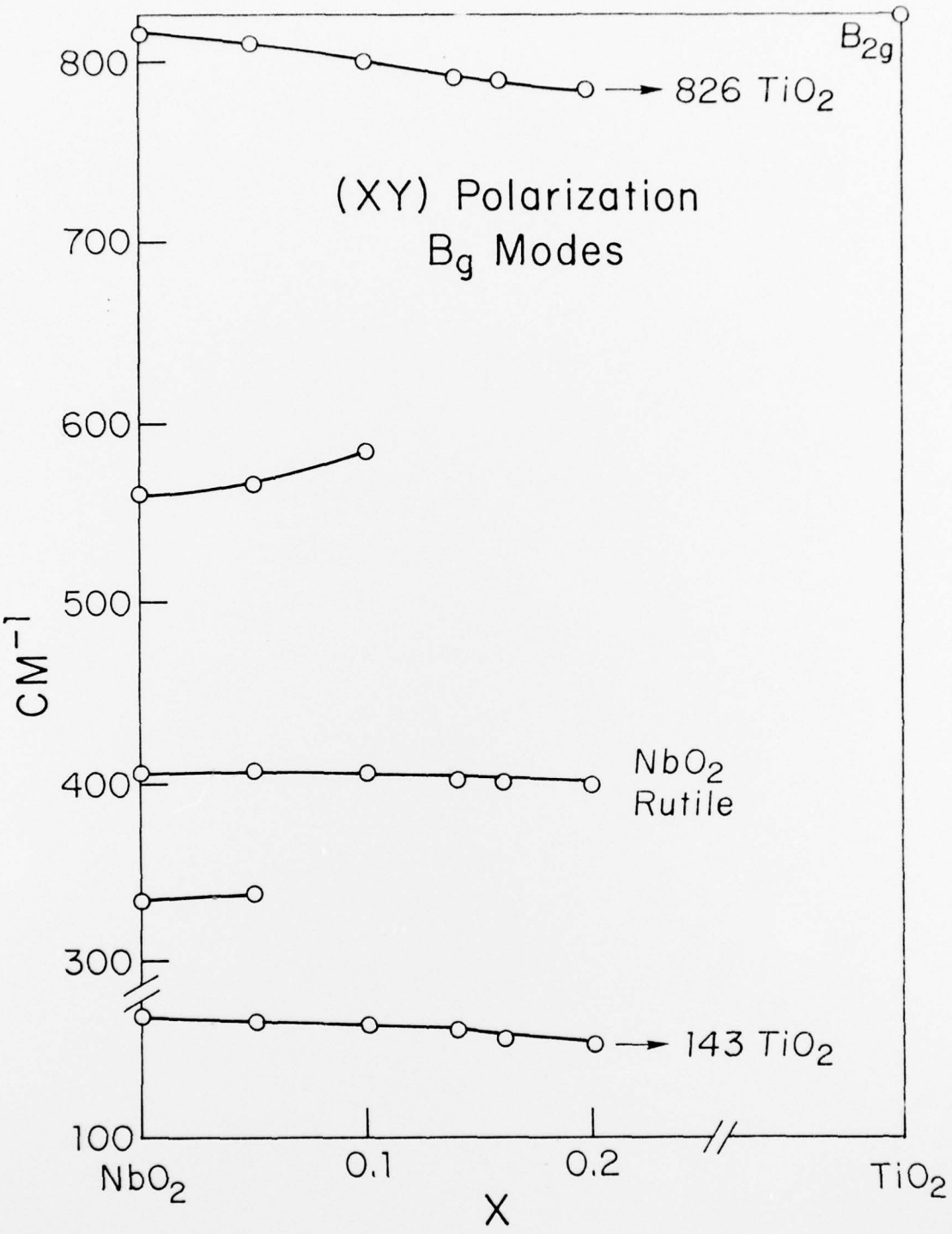
800
700
600
500
400
300
100
CM⁻¹
B2g
826 TiO2
(XY) Polarization
Bg Modes
NbO2
Rutile
143 TiO2
NbO2
0.1
0.2
TiO2
X

Fig. 9

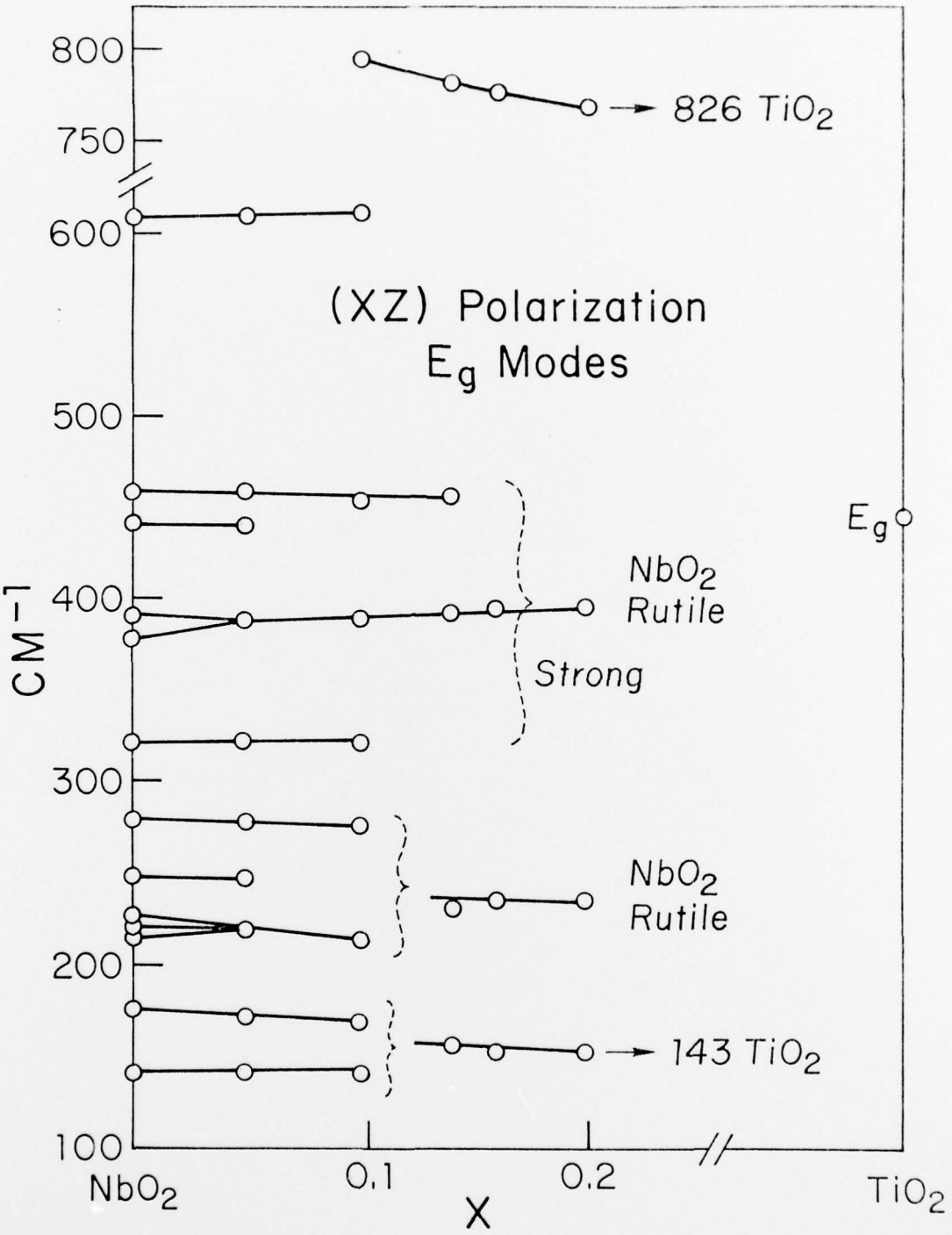
800
750
600
500
400
300
200
100
CM⁻¹
826 TiO2
(XZ) Polarization
Eg Modes
Eg
NbO2
Rutile
Strong
NbO2
Rutile
143 TiO2
NbO2
0.1
0.2
X
TiO2

Fig. 10

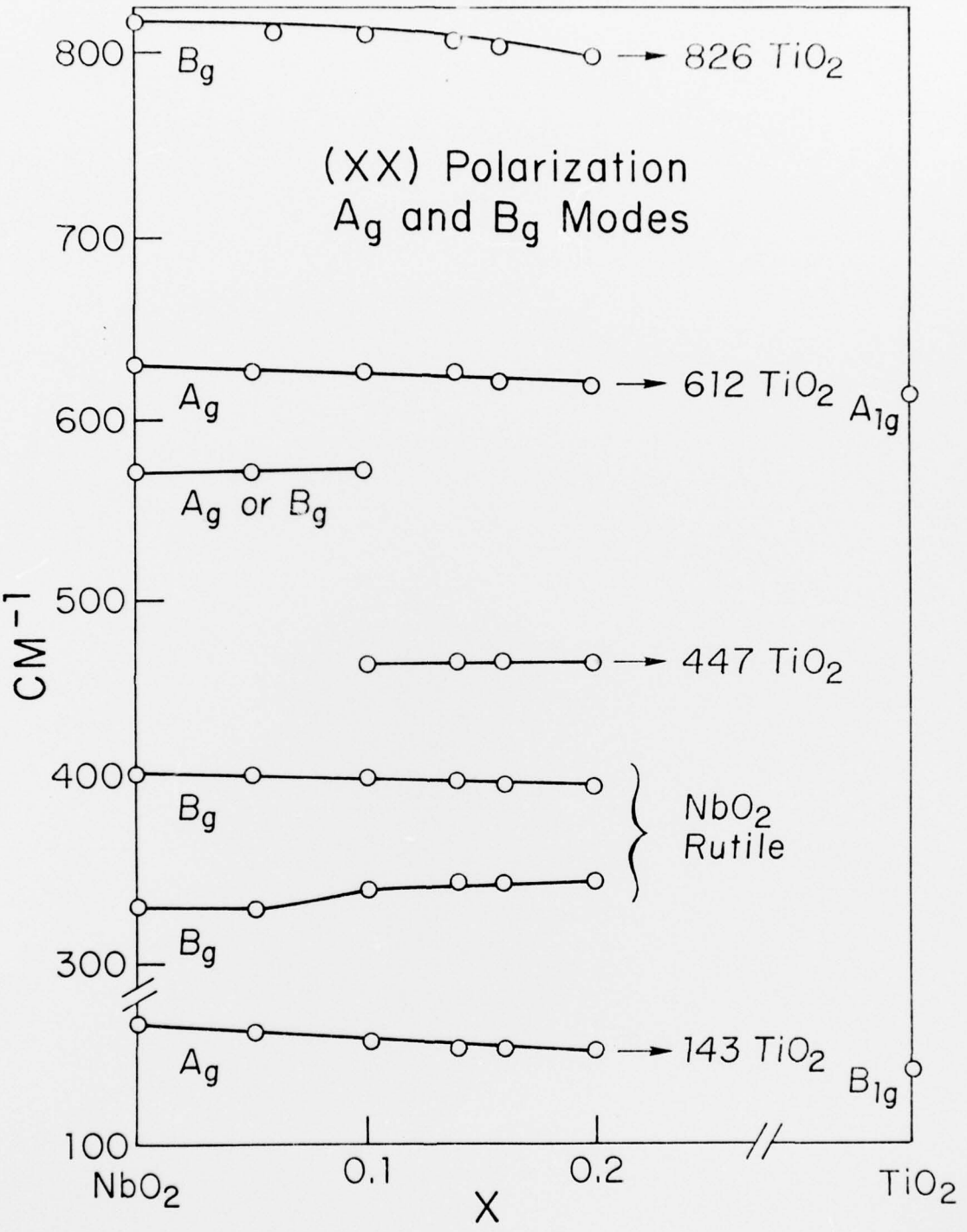
800
700
600
500
400
300
100
CM⁻¹
Bg
826 TiO2
(XX) Polarization
Ag and Bg Modes
Ag
612 TiO2
A1g
Ag or Bg
447 TiO2
Bg
NbO2
Rutile
Bg
Ag
143 TiO2
B1g
NbO2
0.1
0.2
X
TiO2